

REPORT DOCUMENTATION PAGE			Form Approved OMB NO. 0704-0188		
<p>The public reporting burden for this collection of information is estimated to average 1 hour per response, including the time for reviewing instructions, searching existing data sources, gathering and maintaining the data needed, and completing and reviewing the collection of information. Send comments regarding this burden estimate or any other aspect of this collection of information, including suggestions for reducing this burden, to Washington Headquarters Services, Directorate for Information Operations and Reports, 1215 Jefferson Davis Highway, Suite 1204, Arlington VA, 22202-4302. Respondents should be aware that notwithstanding any other provision of law, no person shall be subject to any penalty for failing to comply with a collection of information if it does not display a currently valid OMB control number.</p> <p>PLEASE DO NOT RETURN YOUR FORM TO THE ABOVE ADDRESS.</p>					
1. REPORT DATE (DD-MM-YYYY) 23-03-2009		2. REPORT TYPE Technical Report		3. DATES COVERED (From - To) 1-Jun-2005 - 31-May-2008	
4. TITLE AND SUBTITLE Normalized Implicit Radial Models for Scattered Point Cloud Data without Normal Vectors			5a. CONTRACT NUMBER W911NF-05-1-0301		
			5b. GRANT NUMBER		
			5c. PROGRAM ELEMENT NUMBER 611102		
6. AUTHORS Gregory M. Nielson			5d. PROJECT NUMBER		
			5e. TASK NUMBER		
			5f. WORK UNIT NUMBER		
7. PERFORMING ORGANIZATION NAMES AND ADDRESSES Arizona State University Office of Research & Sponsored Projects Administration Arizona State University Tempe, AZ 85287 -3503			8. PERFORMING ORGANIZATION REPORT NUMBER		
9. SPONSORING/MONITORING AGENCY NAME(S) AND ADDRESS(ES) U.S. Army Research Office P.O. Box 12211 Research Triangle Park, NC 27709-2211			10. SPONSOR/MONITOR'S ACRONYM(S) ARO		
			11. SPONSOR/MONITOR'S REPORT NUMBER(S) 48402-MA.10		
12. DISTRIBUTION AVAILABILITY STATEMENT Approved for public release; federal purpose rights					
13. SUPPLEMENTARY NOTES The views, opinions and/or findings contained in this report are those of the author(s) and should not be construed as an official Department of the Army position, policy or decision, unless so designated by other documentation.					
14. ABSTRACT We describe some new methods for obtaining a mathematical representation of a surface that approximates a scattered point cloud, $\{(x y z) \in N\} \text{ i i i } , , = 1,L$, without the use or need of normal vector data. The fitting surface is defined implicitly as the level set of a field function which is a linear combination of trivariate radial basis functions. Optimal approximations are based upon normalized least squares criteria which lead to eigenvalue/eigenvector characterizations. The normalized aspect allows for the exclusion of the need of normal					
15. SUBJECT TERMS Surface fitting, point clouds, implicit least squares, isosurfaces, noisy 3D data, scattered data approximation					
16. SECURITY CLASSIFICATION OF:		17. LIMITATION OF ABSTRACT		15. NUMBER OF PAGES	19a. NAME OF RESPONSIBLE PERSON
a. REPORT U	b. ABSTRACT U	c. THIS PAGE U	SAR		Gregory Nielson
					19b. TELEPHONE NUMBER 480-965-2785

Report Title

Normalized Implicit Radial Models for Scattered Point Cloud Data without Normal Vectors

ABSTRACT

We describe some new methods for obtaining a mathematical representation of a surface that approximates a scattered point cloud, $\{(x_i, y_i, z_i) \mid i = 1, \dots, N\}$, without the use or need of normal vector data. The fitting surface is defined implicitly as the level set of a field function which is a linear combination of trivariate radial basis functions. Optimal approximations are based upon normalized least squares criteria which lead to eigenvalue/eigenvector characterizations. The normalized aspect allows for the exclusion of the need of normal vector estimates which is one of the unique features of this new method. Localizing techniques are introduced to allow for the efficient application of these new methods to large data sets. The use of a variety of radial basis functions are introduced through various examples that illustrate the performance and efficiency of the new methods.

Normalized Implicit Radial Models for Scattered Point Cloud Data without Normal Vectors

Gregory M. Nielson, Tempe

Abstract

We describe some new methods for obtaining a mathematical representation of a surface that approximates a scattered point cloud, $\{(x_i, y_i, z_i) \mid i = 1, \dots, N\}$ without the use or need of normal vector data. The fitting surface is defined implicitly as the level set of a field function which is a linear combination of trivariate radial basis functions. Optimal approximations are based upon normalized least squares criteria which lead to eigenvalue/eigenvector characterizations. The normalized aspect allows for the exclusion of the need of normal vector estimates which is one of the unique features of this new method. Localizing techniques are introduced to allow for the efficient application of these new methods to large data sets. The use of a variety of radial basis functions are introduced through various examples that illustrate the performance and efficiency of the new methods

Key Words: Surface fitting, point clouds, implicit least squares, isosurfaces, noisy 3D data, scattered data approximation

1. Problem, Introduction and Motivation

We present a new technique for modeling a scattered point cloud data, $\{(x_i, y_i, z_i) \mid i = 1, \dots, N\}$. Based upon least squares error criteria the method determines the parameters of an implicit model, $F(x, y, z)$, so that the zero level contour surface, $\{(x, y, z) : F(x, y, z) = 0\}$ yields a surface that approximates the point cloud. One of the unique features of this new method is the lack of the need of normal vector estimation. Estimating normal vectors (including orientation) can be problematic and error prone and so it is rather beneficial if this process can be avoided. Prior to proceeding to the details of describing our new method, we give a brief overview of point cloud fitting techniques which establishes the context and provides motivation.

One of the first things that we should point out is that the problem of point cloud fitting should be distinguished from that of scattered data modeling [11, 12, 21]. Even though many of the basic techniques and tools from CAGD (Computer Aided Geometric Design) and multivariate approximation theory apply to both problems, they are basically different. The problem of scattered data modeling is concerned with methods of

producing a bivariate function $F(x, y)$ such that $F(x_i, y_i) \approx z_i$. That is, for the traditional scattered data modeling there is the assumption that the data consists of samples taken from the surface graph of a bivariate function. One fundamental connection between the two problems is through some type of parameterization of the point cloud [8, 9] whether this be implicit or explicit. The term “scattered data” was coined by Schumaker in his 1976 paper and there was a great deal of interest and published research on (mainly) bivariate problems in the 70s and 80s. With the advent of scientific visualization along with volume visualization in the 90s, there was growing interest in trivariate scattered data modeling [21] and interest in this area continues to grow. In many respects, the problem of point cloud fitting is more difficult because it is less understood, but the widespread and strong need (see [20]) for practical and effective methods make this an important problem.

A number of methods involve the signed distance function (see [14]), $D(P)$, which is a trivariate function defined to be zero on the surface S , negative interior to S and positive outside of S . The surface is extracted from $D(P)$ as a triangular mesh surface approximation to the zero level isosurface. Typically, $D(P)$ is sampled on a 3D rectilinear grid and a method like the marching cubes algorithm [22] is used. Once it is decided what the metric or the definition of distance from a surface to a point cloud is to be, it is usually not too difficult to develop algorithms for the efficient computation of the distance function. The particular difficulty here is getting the sign right; that is, to be able to efficiently and effectively determine when a point is inside the surface or outside. Typical of the methods based upon distance functions is that of [15], where the sign is based upon local least squares estimates of the normal vector of the surface and a consistent orientation (in or out) is sought with the Riemannian map estimate. One of the drawbacks to this method is the heuristics of the signed distance function calculation may lead to gaps in the surface and the difficulty of choosing the proper resolution for the marching cubes voxel grid can have detrimental effects on the success of the method.

Another important concept involved in point cloud fitting problems is the Delaunay tetrahedrization and its dual, the Dirichlet tessellation and Voronoi diagram. The method based upon alpha shapes of [6] is a typical and early example. Here the first step is the Delaunay tetrahedrization. The second step is to apply the alpha-erasure to remove tetrahedra, triangles and edges whose minimum surrounding sphere is not contained in the alpha-erasure sphere. The result is called the alpha-shape. In the third step, triangles for the final surface are selected so that a sphere of radius alpha containing the triangle does not contain any other point cloud points. The main negative aspect of this approach is the choice of a suitable value of alpha. Too big of a choice leads to poor approximations not utilizing many of the points of the point cloud and too small a choice leads to gaps and fragmented surfaces. We mention another potential drawback to these types of methods for certain applications. The resulting triangular mesh surface has vertices that are points of the original point cloud. For noisy data or overlapping data resulting from imperfect registration of scanned data, this may be undesirable. Rather than interpolated the point cloud (or a subset), it is potentially more desirable to approximate it for some applications.

Another class of methods obtains a triangle mesh surface (TMS) approximation to the point cloud by deforming an initial approximation using metrics that measure the distance between the point cloud and the TMS with possible refinement of the TMS. Representative examples of such methods include [7] and [24]. Adaptive techniques allow fitting methods to efficiently apply more resources to regions of higher complexity (see [1], [2]).

2.0 Normalized Implicit Eigen-value/vector Least Squares Models

Given a collection of scattered points $P_i, i=1, \dots, N$ we are interested to find a field function $F(P)$ of an implicitly define model so that zero level contour, $\{(x, y, z): F(x, y, z)=0\}$, represents an approximation to the data in the sense that $F(P_i) \approx 0, i=1, \dots, N$. We assume that the fitting function F is spanned by the basis functions, $B_j(P), j=1, \dots, M$ and that the least squares criteria is used and so we consider the problem:

$$\min_{F_j} \sum_{i=1}^N \left[\sum_{j=1}^M F_j B_j(x_i, y_i) \right]^2 .$$

Without additional constraints, this problem is not well formulated since an optimal fit is the identically zero function. We add the additional constraint of normalizing the weights/coefficients of the fitting function and consider the modified optimization problem:

$$\min_{F_j} \left\{ \sum_{i=1}^N \frac{\left[\sum_{j=1}^M F_j B_j(P_i) \right]^2}{\sqrt{\sum_{j=1}^M F_j^2}} \right\} . \quad (1)$$

We now set out to find the characterizing equations for the minimizing set of coefficients, $F_j, j=1, \dots, M$. While it is possible to invoke some general results concerning Rayleigh quotients (see [16]) it is both interesting and instructive to proceed using conventional calculus techniques. To this end, we introduce the following notation for the objective function of (1),

$$\phi(F_1, F_2, \dots, F_M) = \frac{\sum_{i=1}^N \left[\sum_{j=1}^M F_j B_j(P_i) \right]^2}{\sum_{j=1}^M F_j^2} . \quad (2)$$

A minimizer of ϕ , necessarily must be a stationery point; that is, a root of the gradient, which requires that

$$\nabla\phi(F_1, F_2, \dots, F_M) = 0 = \begin{pmatrix} \frac{\partial\phi(F_1, F_2, \dots, F_M)}{\partial F_1} \\ \vdots \\ \frac{\partial\phi(F_1, F_2, \dots, F_M)}{\partial F_M} \end{pmatrix}. \quad (3)$$

Using the standard calculus quotient rule for derivatives, we have

$$\frac{\partial\phi}{\partial F_k} = \frac{\|F\|^2 \left\{ \sum_{i=1}^N \left(2 \left[\sum_{j=1}^M F_j B_j(P_i) \right] B_k(P_i) \right) \right\} - \left\{ \sum_{i=1}^N \left[\sum_{j=1}^M F_j B_j(P_i) \right]^2 \right\} 2F_k}{\|F\|^4} = 0,$$

where $\|F\|^2 = \sum_{j=1}^M (F_j)^2$.

It is easy to see that the above system of equations is equivalent to

$$A \begin{pmatrix} F_1 \\ F_2 \\ \vdots \\ F_M \end{pmatrix} - \frac{\sum_{i=1}^N \left[\sum_{j=1}^M F_j B_j(P_i) \right]^2}{\|F\|^2} \begin{pmatrix} F_1 \\ F_2 \\ \vdots \\ F_M \end{pmatrix} = 0, \quad (4)$$

where $A = BB^*$ denotes the gram matrix and

$$B = \begin{pmatrix} B_1(P_1) & B_1(P_2) & \dots & B_1(P_N) \\ B_2(P_1) & B_2(P_2) & \dots & B_2(P_N) \\ \vdots & \vdots & \ddots & \vdots \\ B_M(P_1) & B_M(P_2) & \dots & B_M(P_N) \end{pmatrix}. \quad (5)$$

At this point, we assume that the data, $P_i, i=1, \dots, N$ and the basis functions $B_j, j=1, \dots, M$ are such that A is positive definite. From Equation (4), we can see that minimizing solution, F must be an eigenvector of A . If we let λ be the associated eigenvalue then we may also conclude that

$$\frac{\sum_{i=1}^N \left[\sum_{j=1}^M F_j B_j(P_i) \right]^2}{\sum_{j=1}^M F_j^2} = \lambda$$

and so we have established the fact that the vector F that minimizes (2) is the eigenvector of the gram matrix, BB^* associated with its smallest eigenvalue.

2.1 Proof of Concept Example

We now present a very simple example which illustrates the fitting process and which can be subsequently used by others to check and verify concepts and implementations. Here we have thirteen (13) data points: (0.44, 0.13), (0.24, 0.15), (0.22, 0.35), (0.31, 0.49), (0.35, 0.60), (0.43, 0.70), (0.51, 0.77), (0.57, 0.70), (0.70, 0.55), (0.85, 0.30), (0.88, 0.23), (0.80, 0.10), (0.60, 0.10) which are depicted in the right image of Figure 1. We use a set of basis functions which give rise to the general model

$$F(x, y) = a + bx + cy + \sum_{j=1}^M F_j e^{-R\|P-Q_j\|^\mu}$$

where $P = (x, y)$ and $Q_j, j = 1, \dots, M$ are the “knots” for the exponential radial basis functions. For this particular example, we simply choose $R = 1$, $\mu = 1$, $M = 3$ and knot values $Q_1 = (0.5120, 0.6640)$, $Q_2 = (0.7825, 0.1825)$ and $Q_3 = (0.3025, 0.2800)$. These knots are selected according to the “venetia criteria” which is explained below, but basically this means that these three knots are the “closest” three points to the data points $\{P_i\}_{i=1}^{13}$. This requires that each knot be the centroid of the data points lying in its Voronoi/Dirchlet cell/tile. For this particular case, we have $Q_1 = (P_5 + P_6 + P_7 + P_8 + P_9)/5$, $Q_2 = (P_{10} + P_{11} + P_{12} + P_{13})/4$, $Q_3 = (P_1 + P_2 + P_3 + P_4)/4$ and

$$BB^* = \begin{pmatrix} 13.00 & 6.90 & 5.17 & 9.22 & 8.79 & 9.01 \\ 6.90 & 4.28 & 2.61 & 4.79 & 5.00 & 4.50 \\ 5.17 & 2.61 & 2.80 & 4.12 & 3.18 & 3.48 \\ 9.22 & 4.79 & 4.12 & 6.82 & 6.03 & 6.34 \\ 8.79 & 5.00 & 3.18 & 6.03 & 6.21 & 5.99 \\ 9.01 & 4.50 & 3.48 & 6.34 & 5.99 & 6.41 \end{pmatrix}.$$

The smallest eigenvalue of BB^* is 0.00273142 leading to the solution

$$F(x, y) = 0.740 + 0.088x - 0.093y - .258e^{-\|P-Q_1\|} - 0.526e^{-\|P-Q_2\|} - 0.306e^{-\|P-Q_3\|}$$

Which is depicted in Figure 1.

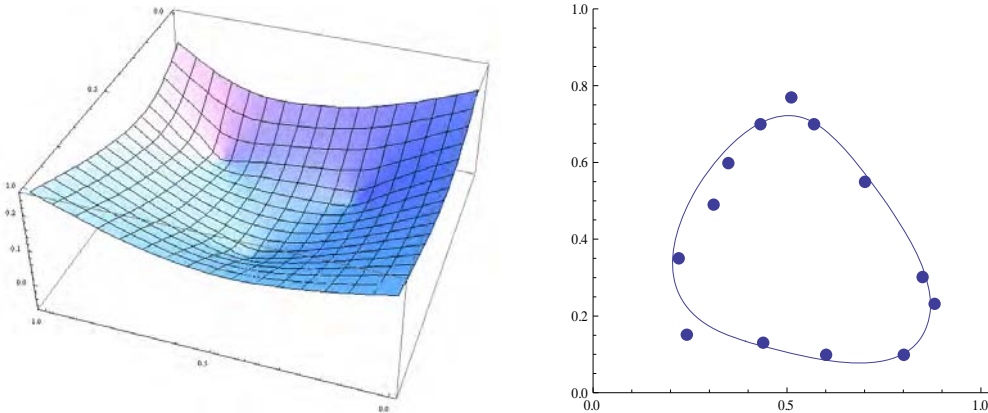


Figure 1. The normalized implicit field function is shown on the left and on the right is shown the zero level contour of this implicit fit along with the input scattered point cloud.

3. Venetia Criteria for Knot Selection.

Some related methods for knot selection have previously been used and discussed in [10], [13], [23], [25]. This method of selecting knots used here is based upon minimizing the distance between the knots $\{Q_j, j=1, \dots, M\}$ and the scattered point cloud, $\{P_i, i=1, \dots, N\}$. This minimal distance requirement leads to the sufficient condition called the “venetia criterion” where Q_j is required to be the centroid of the points lying in its Theissen/Dirichlet region. The Theissen/Dirichlet region is defined to be the set of points closer to Q_j than any other $Q_k, k \neq j$ and is denoted by $T/D[Q_j]$. Computational algorithms for the case of two-dimensions are discussed in [10] and for case of three-dimensions in [25]. These algorithms involve the basic “venetia iteration” where a knot $Q_j^{(K)}$ is updated to a new knot $Q_j^{(K+1)}$ which is the centroid of the data points lying in the Theissen/Dirichlet region of $Q_j^{(K)}$. As it is pointed out in both [10] and [25], this type of iteration quickly converges, but not necessarily always to a global optimal knot set that is a minimal distance to the data points. Nevertheless, we have found that with good initial knot distribution, this type of iteration leads to a very efficient means of determining knot locations which subsequently leads to overall efficient implicit approximation models.

In the example shown in Figure 2, we use as an initial approximation the centroids of the points lying in the lattice grid points of a 3x3 grid. As it turns out two of the nine cells are void of data points and so this approach only leads to seven knots.

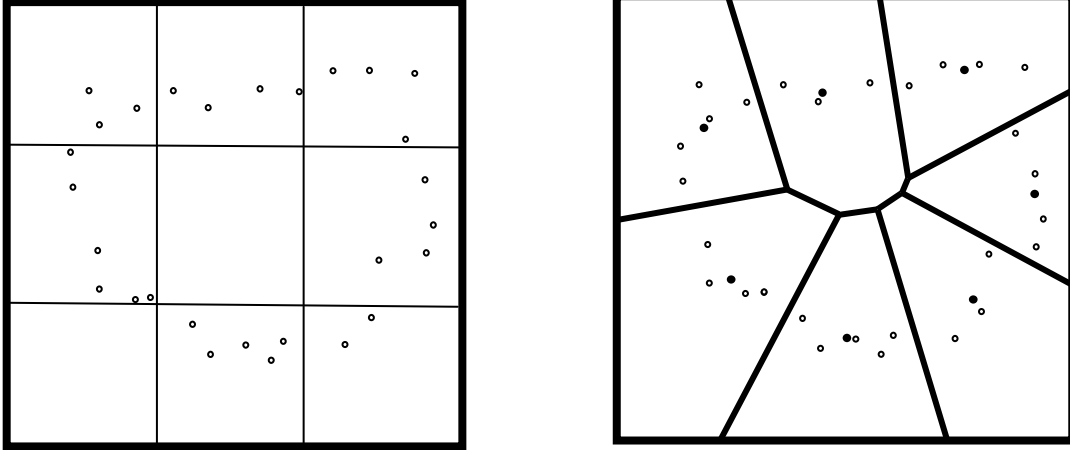


Figure 2. The scattered point cloud is illustrated with “unfilled” circles and the knots are the “filled” circles. The knots in the right image are characterized by the “Venetia Criterion” which is a sufficient condition for minimizing the overall distance between the knots and the scattered point cloud and implies that each knot is the centroid of the data points lying in their respective Theissen/Dirichlet regions. Each of the nine regions of the left image containing data points is “seeded” with a knot prior to the optimization process.

4.0 The Localization Technique

For large data sets, the concepts of localization can be used where the fitting process is broken down into a collection of smaller problems and the final model is a blend of these local smaller and simpler fitting problems. This general technique is described in [21]. The basic ideas of the technique were also used by [26] where they refer to Franke & Nielson [11] as their original source for the basic idea. Here, we give a brief, high level, overview of this technique within the context of scattered data interpolation. Input to the problem of scattered data modeling consists of a collection of scattered data point locations $P_i, i = 1, \dots, N$ contained in the domain D and associated dependent data values $Y_i, i = 1, \dots, N$. It is desired to construct an interpolating function F defined over D that has the property, $F(P_i) = Y_i, i = 1, \dots, N$. Let $W_k, k = 1, \dots, M$ be a collection of functions defined over D and further assume that each W_k has local support. That is the set of points P_j such that $W_k(P_j) \neq 0$ is a small subset of the total number of N points and the every data point must lie in the support of some W_m . Also it must be the case that

$\sum_{k=1}^M W_k(P) \equiv 1$ for all points P in the composite domain. Note that this last condition is not a deal breaker for if it is not satisfied, then it is possible to use the “normalized” weight functions $w_k = \frac{W_k}{\sum W_k}$ which do have this sum-to-unity property. Assume we

have a collection of local interpolating functions $F_k(P)$ each having the property that $F_k(P_i) = Y_i$ for all P_i in the support of $F_k(P)$, then the composite weighted model

$F(P) = \sum_{k=1}^M W_k(P) F_k(P)$ has the property that

$$F(P_i) = \sum_{k=1}^M W_k(P_i) F_k(P) = Y_i, \text{ for all } i = 1, \dots, N.$$

Here we are not solving an interpolation problem, but rather a least squares approximation and also we are not doing conventional scattered data interpolation (i. e. $F_k(P_i) = Y_i$), but yet, we can still exploit these basic ideas to make large data set problems tractable with our present approach. We can explain best how this technique works with a simple example with 32 scattered data points as illustrated in Figure 3. We wish to find an implicit model similar to what was accomplished in the previous example of Figure 1, but rather than solve the overall problem, we break it down into some smaller problems and combine the solutions using the techniques of localization. Potential candidates for localizing functions are piecewise bilinear/trilinear functions defined over a user specified $N \times M$ or $N \times M \times K$ grid. Each localizing function W_{ij} has the property that $W_{ij}(k, l) = \delta_{ik} \delta_{jl}$. Since the sum of these localizing functions is a piecewise bilinear (trilinear) which takes on the value 1 at each grid point and the summation is identically equal to 1. For each localizing function, we compute the approximation based upon the data points lying in the support of this localizing function. The final approximation is then the weighted sum of the local approximations. For the example of Figure 3, the domain is the square $[0,3] \times [0,3]$. Actually for this small case where the “exceptional” boundary cases constitute such a large percentage of the cases, we only compute four localized approximations; one each of the four subsets of data lying in the domains $[0,2] \times [0,2]$, $[0,2] \times [1,3]$, $[1,3] \times [0,2]$ and $[1,3] \times [1,3]$. These are respectively referred to as F_{11} , F_{12} , F_{21} and F_{22} . The final result is

$$G(x, y) = (w_{00} + w_{01} + w_{10} + w_{11})F_{11}(x, y) + (w_{02} + w_{03} + w_{12} + w_{13})F_{12}(x, y) \\ + (w_{20} + w_{21} + w_{30} + w_{31})F_{21}(x, y) + (w_{22} + w_{23} + w_{31} + w_{33})F_{22}(x, y) \quad (6)$$

which is illustrated in the two lower images of Figure 3. Using only four approximations here rather than 16 serves to point out the possibility of other data dependant consolidations to be used for localization that are based upon rectilinear grids. There are a large number of potentially interesting and useful options to consider and exploit in this context.

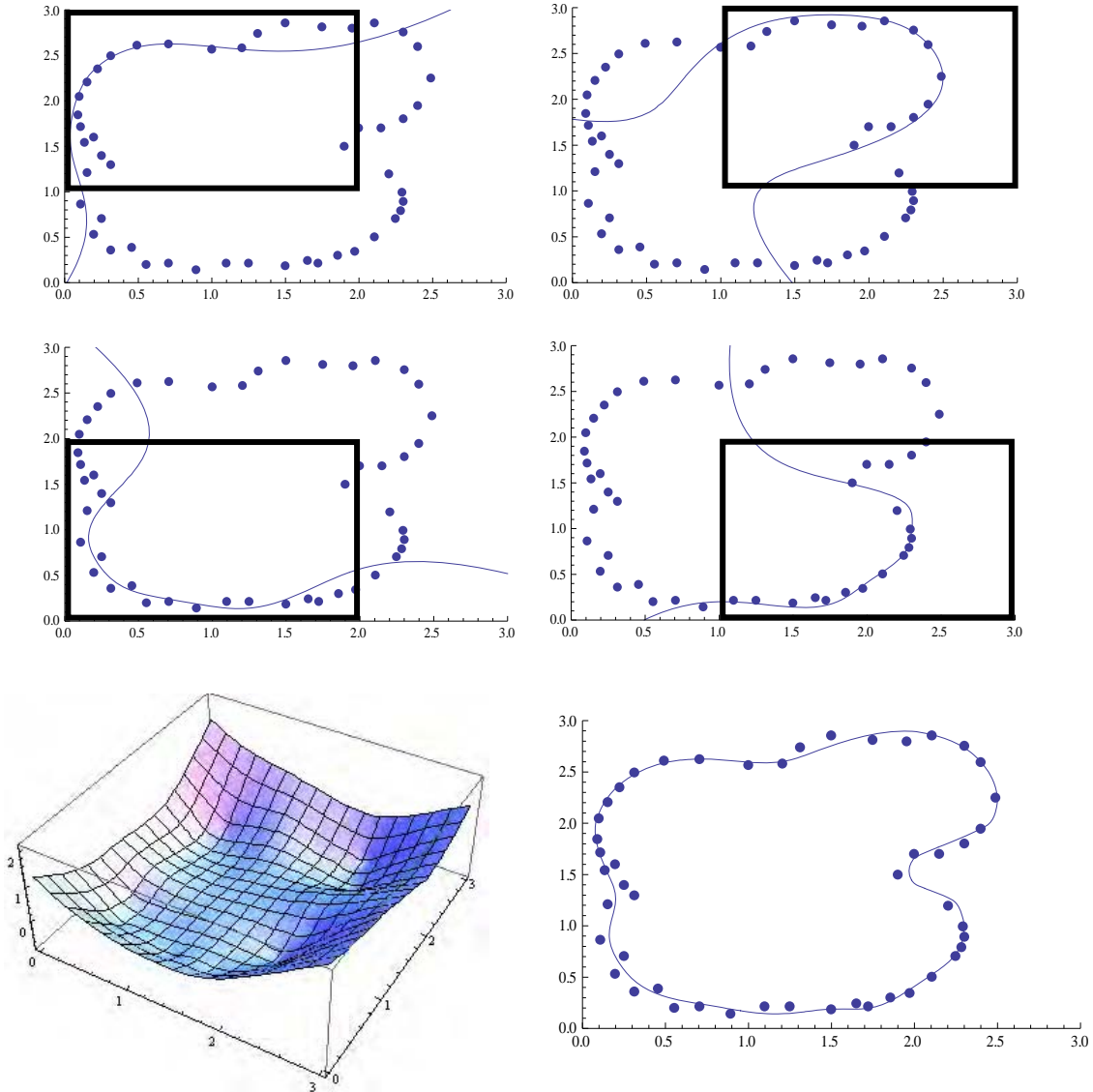


Figure 3. An example that illustrates the localization process. The upper four graphs show the data and the contour of the normalized implicit model applied to the data contained in bounded rectangular region respectively. These regions constitute the support of the localizing functions being used. The two images in the bottom row show the final blend of these four local approximations. The blending functions are piecewise bilinear functions which take on 0 or 1 at each of the integer lattice domain points and have support on the respective rectangles. The lower, left image is the global normalized implicit model and the lower, right image shows the zero level contour along with the input scattered point cloud. It is really very interesting that the quality of the fit is so good even without the use of normal vector (orientation) information.

5. Examples and Applications

5.1 Parameter specification for least squares parametric curve fitting

This first example is a typical representative of a 2D curve fitting problem where we are given a collection of points $(x_i, y_i), i=1, \dots, N$ and it is desired to fit a curve that approximates the shape inferred by these points. Since the data does not necessarily infer

a function relationship, $y = F(x)$, parametric methods $(x(t), y(t)) 0 \leq t \leq 1$ can be used. Most any approach based upon parametric curves will require the specification of associated parameter values t_i for each scattered point (x_i, y_i) . For this example we will use least squares fitting and so once the parameter values are specified, the linear, least squares fitting problem is rather straight forward:

$$\min_{\{c_k\}} \sum_{i=1}^N \left(\sum_{k=1}^M c_k B_k(t_i) - p_i \right)^2 \quad (7)$$

where $\{B_1, B_2, \dots, B_M\}$ are the basis functions, $p_i = (x_i, y_i)$ are the points of the scattered point cloud, $c_k, k = 1, \dots, M$ are the to be determined coefficients of the final fitting model and $t_i, i = 1, \dots, N$ are the all-important parameter values which have yet to be specified. Once these parameter values are specified, solving the minimization problem of (7) has been studied extensively and there are many efficient and effective computational methods generally available. If these parameter values are not known, but the scattered data points are at least ordered, then there are available a number of rather effective means for determining parameter values. If we choose to not specify these values, then, it is possible that these values can be left undetermined and simply be added to the unknowns for the minimization process. This makes the least squares problem nonlinear and extremely problematic. Here, we suggest using the implicit methods as a basis for selecting these parameter values. In a nutshell, the approach is as follows. First an implicit model as we have described here is fit to the data points (x_i, y_i) . Next the data points are projected onto the contour of the implicit model. These values are ordered by there projections onto the zero level contour. This ordering (and possibly the relative distances along the contour) is used to determine the parameter values. In the example of Figure 4, we use an approximate projection of each data point onto the contour of the implicit model. The projection is taken to be the intersection of the contour and the parametric line

$$L(t) = (x_i, y_i) + t \left[\frac{\partial F}{\partial x}(x_i, y_i), \frac{\partial F}{\partial y}(x_i, y_i) \right].$$

Depending upon the details of how F is stored and/or represented, the gradient may or may not be immediately available. If not, discrete approximations can be used.

For the example of Figure 4, we have 70 scattered data points. An implicit model, similar to that of Figure 3 is fit to these points. The data and the fit are shown in the top image of Figure 4. Each of the data points is projected onto the contour of the implicit model. These projected points give a relative order for the data points which is used to obtain the associated parameter values $\{t_i\}_{i=1}^{70}$. Based upon these parameter values, a periodic, parametric cubic spline is fit to the airfoil data in the least squares sense. The result is shown in the bottom image of Figure 4.

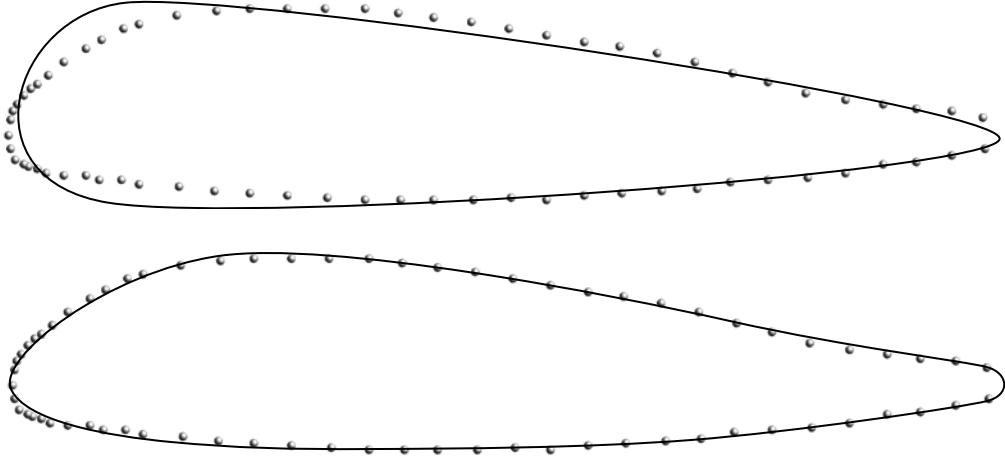


Figure 4. Top image shows airfoil data and NIRM fit. The bottom image shows the least squares parametric spline fit with proportionately spaced knots so that each knot interval has approximately the same number of data point parameter values.

5.2 Boot and Foot CSG Example

This next example utilizes a scattered point cloud data set obtained from scanning a physical boot which is depicted in the left image of Figure 5. There are approximately one million data points. While the point set is fairly uniformly dense, it is rather noisy due to the method of collection which requires only a video projector and a camera (see [27] for example). A 10% sample of the points is shown in the center image of Figure 5. A rendering of the implicit model is shown in the far right image of Figure 5. A localized model using the techniques of Section 4 is used. The grid analogous to the 3×3 grid of Figure 2 is a uniform grid of size $100 \times 100 \times 50$ over the bounding cuboid of the data. The localizing technique of Section 4 is used based upon piecewise, trilinear localizing functions defined over a $50 \times 50 \times 25$ grid. The basis functions are of the form

$$F(x, y, z) = a + bx + cy + dz + \sum_{j=1}^M F_j \left[\frac{R_j - \|P - Q_j\|}{R} \right]_+^{\mu_j}.$$

These basis functions have previously been successfully used in [23]. The value of R is the radius of the support regions of the localizing functions. The power μ is simply set to 2 for this particular example. The knot selection technique described above is seeded with 7 knots per non-empty cell. The final implicit fit is sampled on a 3D rectilinear grid and the dual marching cubes [22] method is used to compute a polygon contour surface.



Figure 5. Left image is photograph of motocross boot. Middle image is rendering of 10% of the approximately one million data points scanned from a physical boot. Right image is a rendering of isosurface extracted from implicit model.

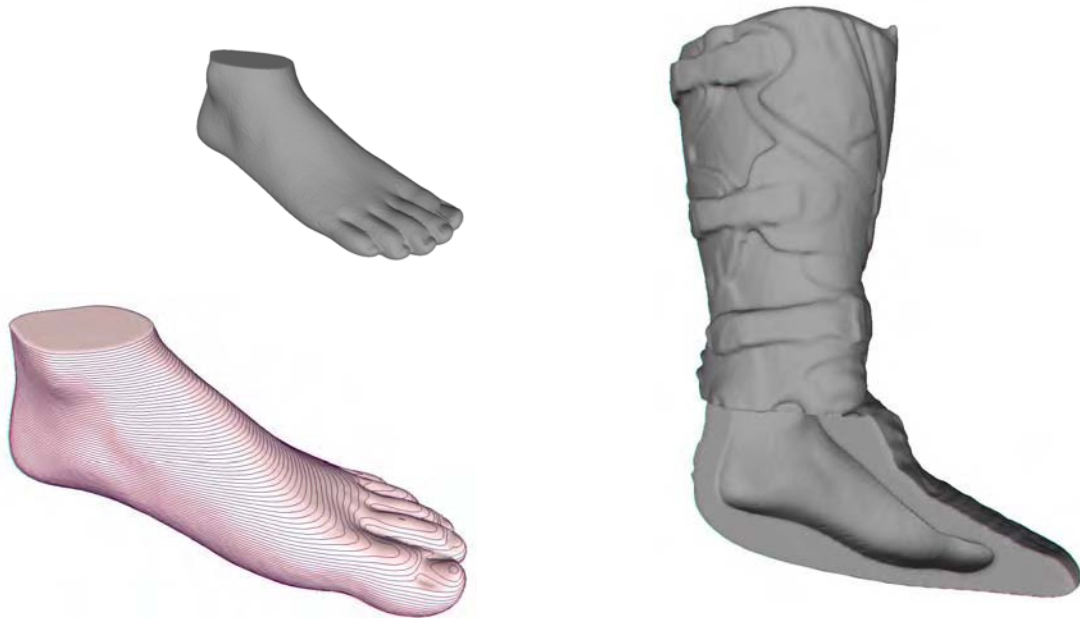


Figure 6. Top left image is contour of implicit model of “noisy foot” data using exponential basis functions. Bottom left is right foot obtained as $F(y, x, z) = 0$. Right image illustrated the results of Boolean operations which are easily accomplished with implicit models.

In Figure 6 we show yet another example. This example utilizes the “noisy foot” data from Geomagic. Here we use the 3D versions of the same exponential basis functions

used in Example 2.1. In the right image we show an example of where the “foot” has been removed from the “boot”. One of the reasons for including this example is to underscore the ease of computing Boolean operations (see [3]) on models that are implicitly defined as is the case for the fitting models of this paper. If we let F_A denote the field function for a point set A whose boundary is a surface of interest. That is $A = \{(x, y, z): F_A(x, y, z) \geq 0\}$. And if B is another three dimensional point set with the field function F_B , then it is easy to see that the union is defined by

$$A \cup B = \{(x, y, z): \text{Max}(F_A(x, y, z), F_B(x, y, z))\} \quad (8)$$

and so we have that $F_{A \cup B} = \text{Max}(F_A, F_B)$. Similarly, we have for the intersection $F_{A \cap B} = \text{Min}(F_A, F_B)$.

6. Remarks

1. Here we have used two classes of radial basis functions. Namely

$$F(x, y, z) = a + bx + cy + dz + \sum_{j=1}^M F_j e^{-R_j \|P - Q_j\|^{\mu_j}} \quad (9)$$

and

$$F(x, y, z) = a + bx + cy + dz + \sum F_j \left[\frac{R_j - \|P - Q_j\|}{R_j} \right]^{\mu_j}. \quad (10)$$

There are a great number of other radial basis functions which could be considered that may have particularly efficient fitting capabilities for certain types of data sets.

2. Using the same data as in the “proof of concept” example of Section 2.1, but with the basis functions of (10) (with $R_j = 1$, $\mu_j = 2 \vee j$), we obtain the results shown in Figure 7. While the contour seems to be a superior fit to that of the earlier example, the criteria of normalized least squares is actually larger for this model. The smallest eigenvalue for example of Figure 1 is .00273 and here the smallest eigenvalue is 0.00767 and so, in a standard least squares sense of measuring error the approximation of Figure 1 is actually better. This seems to indicate that some possible adjustment in the overall fitting criteria may be in order. A shallow field function would lead to a small RMS error, but the distance of the point cloud to the contour surface could still not be small. Normalizing with gradient norms is a possibility, but, of course, we don’t want to destroy the relationship of the solution we have here and its connection to the eigenvalues and eigenvectors. Care must be taken to appropriately alter the fitting norm, but still be able to solve the problem without resorting to the iterative methods of nonlinear least squares fitting. We will report on our progress in this area in a future paper.

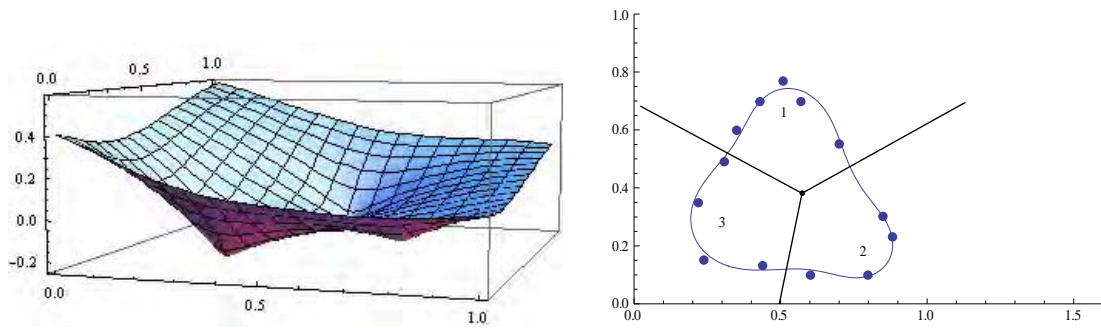


Figure 7. The same point cloud as in the example of Figure 1, but with different radial basis functions. The contour appears to be a better approximation, yet the implicit least squares fit error is larger. This motivates discussion about using a different fitting criteria (error metric). The triad of the right image is the Dirichlet tessellation of the knots which are indicated with numeric values. We note that the knots satisfy the “ventia” criteria in that they are the centroids of the scattered point cloud lying in the respective Dirichlet tiles.

Acknowledgments

We wish to acknowledge the support of the Army Research Office under contract W911NF-05-1-0301. The scanned boot data set is courtesy of T. Tuang and SIDI. The data for the example of Figure 4 is courtesy of G. Farin.

References

- [1] Bertram, M., Barnes, J. C., Hamann, B., Joy, K. K., Pottmann, H., Wushour, W.: Piecewise optimal triangulation for the approximation of scattered data in the plane, *Computer-Aided Geometric Design*, Vol. 17, No. 8, Elsevier, 2000, pp. 767-787.
- [2] Bertram, M., Tricoche, X., Hagen, H.: Adaptive smooth scattered data approximation, *VisSym'03, Joint Eurographics and IEEE TCVG Symposium on Visualization*, 2003, pp. 177-184.
- [3] Bloomenthal, J., Bajaj, C., Blinn, J., Cini-Gascuel, M. P., Rockwood, A., Wyvill, B., Wyvill, G.: *Introduction to Implicit Surfaces*, Morgan Kaufmann, 1999
- [4] Carr, J., Beatson, R., Cherrie, J., Mitchell, T., Fright, W., McCallum, B., Evans, T.: Reconstruction and representation of 3D objects with radial basis functions, *SIGGRAPH '01*, 2001, pp. 67-7
- [5] Cureless, G., Levoy, M.: A volumetric method for building complex models from range images. In: *Proceedings of SIGGRAPH 1996*, ACM Press/ACM SIGGRAPH, New York. *Computer Graphics Proceedings, Annual Conference Series*, ACM, 1996, pp. 303-312
- [6] Edelsbrunner, H., Mücke, E.: Three-Dimensional Alpha Shapes, *ACM Transactions on Graphics* 13, No. 1, 1994, pp. 43-72

- [7] Esteve, J., Brunet, P., Vinacua, A.: Approximation of a variable density cloud of points by shrinking a discrete membrane, *Computer Graphics Forum*, Vol. 24-4, 2005, pp. 791-808
- [8] Floater, M. S., Reimers, M.: Meshless Parameterization and Surface Reconstruction, *Computer Aided Geometric Design* 18, 2001, pp 77-92
- [9] Floater, M. S.: Parameterization of Triangulations and Unorganized Points, In: *Tutorials on Multiresolution in Geometric Modelling*, A. Iske, E. Quak and M. S. Floater (eds.), Springer , 2002, pp. 287-316
- [10] Franke, R., McMahon, J.: Knot selection for least squares thin plate splines, *SIAM Journal on Scientific and Statistical Computing* 13, 1992, pp. 484-498
- [11] Franke, R., Nielson, G.: Smooth interpolation of large sets of scattered data, *International Journal of Numerical Methods in Engineering* 15, 1980, pp. 1691-1704
- [12] Franke, R., Nielson, G.: Scattered data interpolation and applications: A tutorial and survey, In: *Geometric Modelling: Methods and Their Applications*, (Hagen H., Roller, D., eds), Springer, 1990, pp. 131-160
- [13] Franke, R., Hagen, H., Nielson, G.: Least squares surface approximation to scattered data using multiquadratic functions, *Advances in Computational Mathematics* 2, 1994. pp. 81-99
- [14] Frisken, S., R. Perry, Rockwood, A., Jones, T.: Adaptively sampled distance fields: A general representation of shape for computer graphics, *SIGGRAPH '00*, 2000, pp. 249-254
- [15] Hoppe, H., DeRose, T., Duchamp, T., McDonald, J., Stuetzle, W.: Surface reconstruction from unorganized points, In: *Proceedings of SIGGRAPH 1992*, ACM Press/ACM SIGGRAPH, New York. *Computer Graphics Proceedings, Annual Conference Series*, ACM, 1992, pp. 71-78
- [16] Householder, A. S., *The Theory of Matrices in Numerical Analysis*, Blaisdel Publishing Company, New York, 1964
- [17] Mueller, H.: Surface Reconstruction – An introduction, In: *Scientific Visualization* (Hagen, H., Nielson, G., Post, F. eds.), IEEE Computer Society Press, 1999, pp. 239-242
- [18] Nielson, G.: Coordinate-free scattered data interpolation, In: *Topics in Multivariate Approximation*, L. Schumaker, C. Chui, and F. Utreras, Eds., Academic Press, Inc., New Your, New Your, 1987, pp. 175-184.
- [19] Nielson, G.: Modeling and Visualizing Volumetric and Surface-on-Surface Data, In: *Focus on Scientific Visualization*, H. Hagen, H. Mueller, G. Nielson (Eds.) Springer-Verlag, 1993, pp. 191-242.
- [20] Nielson, G.: Challenges in Visualization Research, *IEEE Transactions on Visualization and Computer Graphics*, Vol. 2, No. 2, 1996, pp. 97-99.

- [21] Nielson, G.: Scattered data modeling, *Computer Graphics and Applications* 13, 1003, pp. 60-70
- [22] Nielson, G.: Dual Marching Cubes, *Proceedings of Visualization 2004*, CS Press, 2004, pp. 489-496
- [23] Nielson, G.: Radial Hermite Operators for Scattered Point Cloud Data with Normal Vectors and Applications to Implicitizing Polygon Mesh Surfaces for generalized CSG operations and smoothing, *Proceedings of IEEE Visualization 2004*, 2004, pp. 203-211
- [24] Nielson, G., Hagen, H., Lee, K., Huang, A.: Split & Fit, Adaptive, Least Squares Fitting of Triangular Mesh Surfaces to Scattered Point Cloud Data, In: *Scientific Visualization: The Visual Extraction of Knowledge from Data*, Springer, 2005, ISBN 3-540-26066-8, G. -P. Bonneau, T. Ertl & G. M. Nielson (eds), 2005 pp. 97-112.
- [25] Nielson, G., Hagen, H., Lee, K.: Implicit fitting of point cloud data using radial Hermite basis function, *Computing* Volume 79, No. 3, 2007, pp. 301-307.
- [26] Ohtake, Y., Belyaev, A, Alexa, M. Turk G. Seidel H.-P.: Multi-level partition of unity implicits, *SIGGRAPH 2003*, 2003, pp.123-131
- [27] Yao, Li, Ma, L., Zheng, Z., Wu, D.: A low cost 3D shape measurement method based upon a strip shifting pattern, *ISA Transactions*, Volume 46, Issue 3, June 2007, pp. 267-275